

Original Article



Intravital Two-photon Imaging of Dynamic Alteration of Hepatic Lipid Droplets in Fasted and Refed State

Jieun Moon ,^{1,2} Pilhan Kim ^{1,2,3}

¹Graduate School of Nanoscience and Technology, Korea Advanced Institute of Science and Technology (KAIST), Daejeon, Korea

²KI for Health Science and Technology (KIHST), Korea Advanced Institute of Science and Technology (KAIST), Daejeon, Korea

³Graduate School of Medical Science and Engineering, Korea Advanced Institute of Science and Technology (KAIST), Daejeon, Korea



Received: Mar 18, 2021

Accepted: Jun 22, 2021

Correspondence to

Pilhan Kim

Graduate School of Medical Science and Engineering, Korea Advanced Institute of Science and Technology (KAIST), 291 Daehak-ro, Yuseong-gu, Daejeon 34141, Korea.
E-mail: pilhan.kim@kaist.ac.kr

Copyright © 2021 The Korean Society of Lipid and Atherosclerosis.

This is an Open Access article distributed under the terms of the Creative Commons Attribution Non-Commercial License (<https://creativecommons.org/licenses/by-nc/4.0/>) which permits unrestricted non-commercial use, distribution, and reproduction in any medium, provided the original work is properly cited.

ORCID iDs

Jieun Moon
<https://orcid.org/0000-0002-4523-6979>
Pilhan Kim
<https://orcid.org/0000-0001-8388-1840>

Funding

This work was supported by the Basic Research Program (2020R1A2C3005694) through the National Research Foundation of Korea (NRF) funded by the the Ministry of Science and ICT, Republic of Korea.

Conflict of Interest

The authors have no conflicts of interest to declare.

<https://e-jla.org>

ABSTRACT

Objective: The liver plays a central role in lipid metabolism. During fasting and feeding, the fatty acid trafficking between adipose tissue and liver induces accumulation and dissociation of dynamic hepatic lipid droplets (LDs). Herein, we established an intravital 2-photon imaging technique to longitudinally visualize the dynamic *in vivo* alteration of hepatic LD deposition during fasting and refeeding in the liver of live mouse.

Methods: Intravital 2-photon imaging of liver was performed to observe hepatic LD alteration induced by fasting for different periods of time, 12, 24, and 48 hours followed by refeeding. Hepatic LDs were fluorescently labelled *in vivo* by intravenous injection of Seoul-Flour 44 and visualized by custom-built intravital 2-photon microscope.

Results: Significant increases of the number and size of hepatic LDs were observed by intravital 2-photon imaging of the liver after 12 hours of fasting. The degree of hepatic LD accumulation continuously increased with fasting up to 48 hours. Remarkably, with refeeding for 24 hours, the hepatic LDs accumulated by fasting were fully dissociated and the LD occupancy in the liver was recovered to the normal state.

Conclusion: Utilizing intravital 2-photon microscope with *in vivo* systemic fluorescent labeling of LD in live mice, dynamic alterations of hepatic LDs such as accumulation and dissociation by fasting and refeeding were successfully visualized at a subcellular level *in vivo*. The established method enabling the *in vivo* visualization of LDs will be a useful tool to investigate the pathophysiology of various diseases associated with dysregulated lipid metabolism.

Keywords: Intravital microscopy; Multiphoton microscopy; Lipid droplets; Fasting

INTRODUCTION

The liver is the central organ regulating systemic lipid metabolism affected by nutrient availability and energy demand.¹ During the fed state, the liver uptakes dietary free fatty acids (FAs) and converts FAs to triglycerides (TGs), which can be secreted into plasma as constituents of very low-density lipoproteins. Under a fasting state, the reduced insulin

Author Contributions

Conceptualization: Kim P; Data curation: Moon J; Formal analysis: Moon J; Funding acquisition: Kim P; Investigation: Moon J; Methodology: Moon J, Kim P; Supervision: Kim P; Validation: Kim P; Visualization: Moon J; Writing - original draft: Moon J; Writing - review & editing: Moon J, Kim P.

level stimulates lipolysis in adipose tissue, which leads to a release of free FAs into blood circulation. Released FAs serve as an energy source to the liver, muscle, and heart. In the liver, excessive influx of FAs cause esterification of FAs into TGs in hepatocytes for storage in the form of lipid droplets (LDs). To observe changes in hepatic LD accumulation in a fasted or refeeding state, previous lipid studies²⁻⁶ have mostly relied on conventional histological analysis techniques such as hematoxylin and eosin staining or oil-red O staining of dissected liver tissue from animal models. However, these approaches have provided only cross-sectional information of LD deposition at a single time point, limiting the observation of dynamic change of hepatic LDs during fasting and refeeding.

Intravital microscopy has been actively utilized for *in vivo* observation of dynamic biological phenomena within various tissues in living organisms.^{7,13} Notably, liver function and various cellular-level dynamics in the hepatic microenvironment have been visualized by intravital 2-photon imaging.^{14,15} Nonetheless, high-resolution subcellular-level *in vivo* visualization of hepatic LD dynamics longitudinally in the same mice with intravital 2-photon microscopy has remained a technically challenging task.

In this study, we optimized a custom-built video-rate laser scanning 2-photon microscopy system for intravital 2-photon imaging of hepatic LDs in a live mouse model with a newly developed fluorophore, Seoul-Fluor 44 (SF44), for selective labeling of cellular LDs. Alteration of hepatic LDs induced by fasting for different periods of time, 12, 24, and 48 hours, followed by refeeding, was longitudinally visualized *in vivo*. After 12 hours of fasting, the number and the size of hepatic LDs significantly increased. Accumulation of hepatic LDs continuously increased with fasting up to 48 hours. Remarkably, the hepatic LDs accumulated by fasting were fully degraded after refeeding for 24 hours. The method established in this study for the longitudinal intravital 2-photon imaging of LDs provides a useful technique to study pathophysiology of various human diseases associated with dysregulated lipid metabolism.

MATERIALS AND METHODS

1. Animal model

All animal experiments were performed in accordance with the health guidelines for the use of experimental animals and were approved by the Institutional Animal Care and Use Committee of Korea Advanced Institute of Science and Technology (protocol No. KA-2018-78). Male C57BL/6 mice (OrientBio, Seongnam, Korea) aged 8 weeks were used for all experiments. Before experiments, all mice were maintained in independently ventilated, temperature & humidity-controlled cages (22.5°C, 52.5%) under 12:12 hours light:dark cycle and provided with standard diet and water ad libitum. To observe effects of fasting in hepatocyte, mice were fasted for different period of time; 12, 24, 48 hours and refed for 24 hours. The control mice were continuously fed without fasting. Two mice were used for each experiment group.

2. Imaging system

To visualize the hepatic LDs in the liver *in vivo*, a custom-built laser-scanning 2-photon microscopy system was used (Fig. 1A). A tunable fs-pulse Ti:Sapphire laser (Chameleon Vision S; Coherent, Santa Clara, CA, USA) was used as laser source for 2-photon excitation. Half-wave plate combined with polarizer were used to control the laser intensity. Raster-pattern laser-

scanning was achieved by using a rotating polygonal mirror (MC-5; Lincoln Laser, Tecumseh, Canada) for x-axis scanning and a galvanomirror (6230H; Cambridge Technology, Bedford, MA, USA) for y-axis scanning as previously described.^{1143,1618} 4f lens system was implemented by using anti-reflection coated achromatic lenses (L1:50mm FL, 49356INK, L2:100mm FL, 49360INK, L3:75mm FL, 49358INK, L4:200mm FL, 49364INK; Edmund Optics, Barrington, NJ, USA). The scanning laser beam was delivered to the liver of anesthetized mouse through commercial high numerical aperture objective lens (CFI75ApoLWD25XW, NA 1.1; Nikon, Tokyo, Japan). Fluorescence signals were collected by the objective lens in epi-detection manner and reflected by dichroic beam splitters (DBS1:FF705-Di01; Semrock, Rochester, NY, USA) toward fluorescence detectors (PMT: photomultiplier tube, R7518; Hamamatsu, Iwata, Japan). Shortpass filter (SPF:FF720/SP; Semrock) was used to block the excitation fs-pulse laser. For simultaneous multi-color imaging, the collected fluorescence signals were further spectrally separated by dichroic beam splitters (DBS2:FF495-Di03, DBS3: FF555-Di02; Semrock) and then filtered by bandpass filters (BPF1:FF01-445/20, BPF2:FF01-525/45, BPF3:FF01-585/40; Semrock). Electronic signals from the PMTs were acquired by using multi-channel frame grabber (Solios; Matrox, Quebec, Canada) with a custom-written software based on Matrox Imaging Library (MIL9; Matrox).

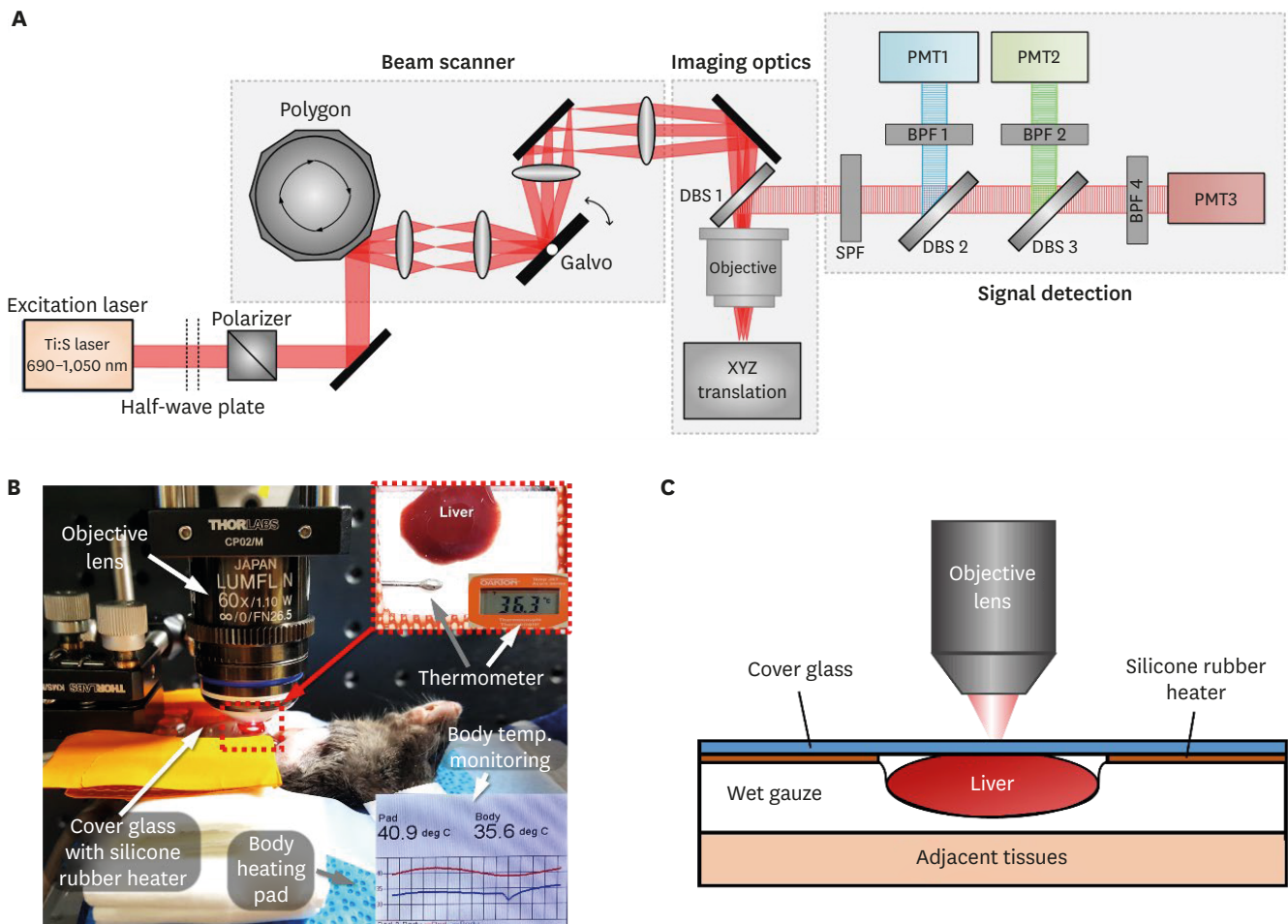


Fig. 1. Intravital microscopy setup to image hepatic lipid droplets in the liver of live mouse. (A) Schematic of custom-built laser scanning 2-photon microscopy system. (B) Photograph of intravital liver imaging setup. Temperature of mouse body and heating pad was continuously monitored. Silicon rubber heater was used for the temperature maintenance of the liver under cover glass. (C) Schematic of liver placement during the intravital liver imaging. BPF, bandpass filter; DBS, dichroic beam splitter; PMT, photomultiplier tube; SPF, Shortpass filter.

3. Intravital imaging of hepatic LD

Mice were anesthetized by intraperitoneal injection of the mixture of Zoletil (20 mg/kg) and Xylazine (11 mg/kg). After the anesthetization, abdominal hair was removed by using hair clipper and hair removal cream. Small incision with size of 10 mm was made on skin and peritoneum. The left lobe of liver was carefully exteriorized and prepared for the intravital imaging (**Fig. 1B**). The cover glass attached with a silicone rubber heater and mini-probe thermometer was placed on the exteriorized liver to monitor and maintain the temperature of local liver tissue constant at 36°C during the intravital imaging. Additionally, a commercial homeothermic heating pad (RightTemp Jr.; Kent Scientific, Torrington, CT, USA) was used to maintain the body temperature of at 36°C during the intravital imaging. A wet gauze soaked with warmed saline was placed between the liver and adjacent tissue to reduce motion artifact (**Fig. 1C**). To avoid dehydration of the surface of the exteriorized liver, warmed saline was continuously supplied to the gauze during the imaging. To fluorescently label hepatic LDs, 120 µL of SF-44 (SPARK Biopharma, Seoul, Korea) solution prepared in Phosphate-Buffered Saline with concentration of 1.67 mM was intravenously injected at 10 minutes before the intravital imaging. During the intravital imaging, the level of anesthetization was periodically monitored by pinching toe. The SF44 accumulated in the hepatic LDs was excited by 2-photon absorption with fs pulse laser beam tuned at 900 nm. The emitted fluorescence was detected by photomultiplier through the bandpass filter with transmission band from 565 nm to 605nm. When the movement was observed, the half of the initial dose of Zoletil and Xylazine mixture was administered by intramuscular injection. To quantify the accumulation and dissociation of hepatic LDs, z-stack images were acquired at randomly selected multiple spots in the liver. Images were acquired by using a 25X water-immersion objective lens (CFI75ApoLWD25XW, NA 1.1; Nikon) providing FOV of 443×443 µm with number of pixels of 1,024×1,024 pixels and pixel size of 0.433 µm. To enhance the signal-to-noise ratio, each image was obtained by averaging 45 frames acquired at video-rate of 15 fps for 3 seconds.

4. Statistical analysis

Acquired z-stack images were converted to 3D-rendered images for quantitative volumetric analysis of hepatic LDs by using commercial image analysis software, IMARIS (Oxford Instruments, Abingdon, UK). By using 'Surface' function of IMARIS, all hepatic LDs in the imaging volume were automatically measured. LDs volume ratio was quantified by dividing total volume of hepatic LDs with total imaging volume. The diameter of individual hepatic LDs was measured by using Image J (NIH, Bethesda, MD, USA). Statistical analysis was performed by using Origin (OriginLab, Northampton, MA, USA). Data are presented as mean±standard deviation. Two mice were analyzed for each experimental group. Statistical differences were determined by 2-tailed unpaired Student's *t*-test. Statistical significance was set at *p*-value less than 0.05.

RESULTS

1. Intravital 2-photon imaging of hepatic LD accumulation induced by fasting

In a fasted condition, the adipose tissue releases a large amount of free FAs and the hepatocytes uptake the FAs and convert them into neutral TGs by esterification to avoid oxidative stress induced by excessive FAs. The synthesized TGs are stored in the form of LDs at the cytoplasm of the hepatocytes. The liver of mice fasted for 12 hours, 24 hours, and 48 hours was imaged *in vivo* following the experimental scheme shown in **Fig. 2A**. The control mice were continuously fed a normal diet ad libitum. The dynamic accumulation of hepatic

LDs by continued fasting was clearly observed in the liver *in vivo* (Fig. 2B). In the liver of control mice without fasting, hepatic LDs were scarcely observed, which occupying only 0.79% of the total imaging volume (Fig. 2C). After only 12 hours of fasting, the number and the size of hepatic LDs significantly increased and the hepatic LD volume ratio also increased substantially to 2.69%–3 times more than the control. After 48 hours of continued fasting, the hepatic LD volume ratio further increased to 5.74%–6 times more than the control.

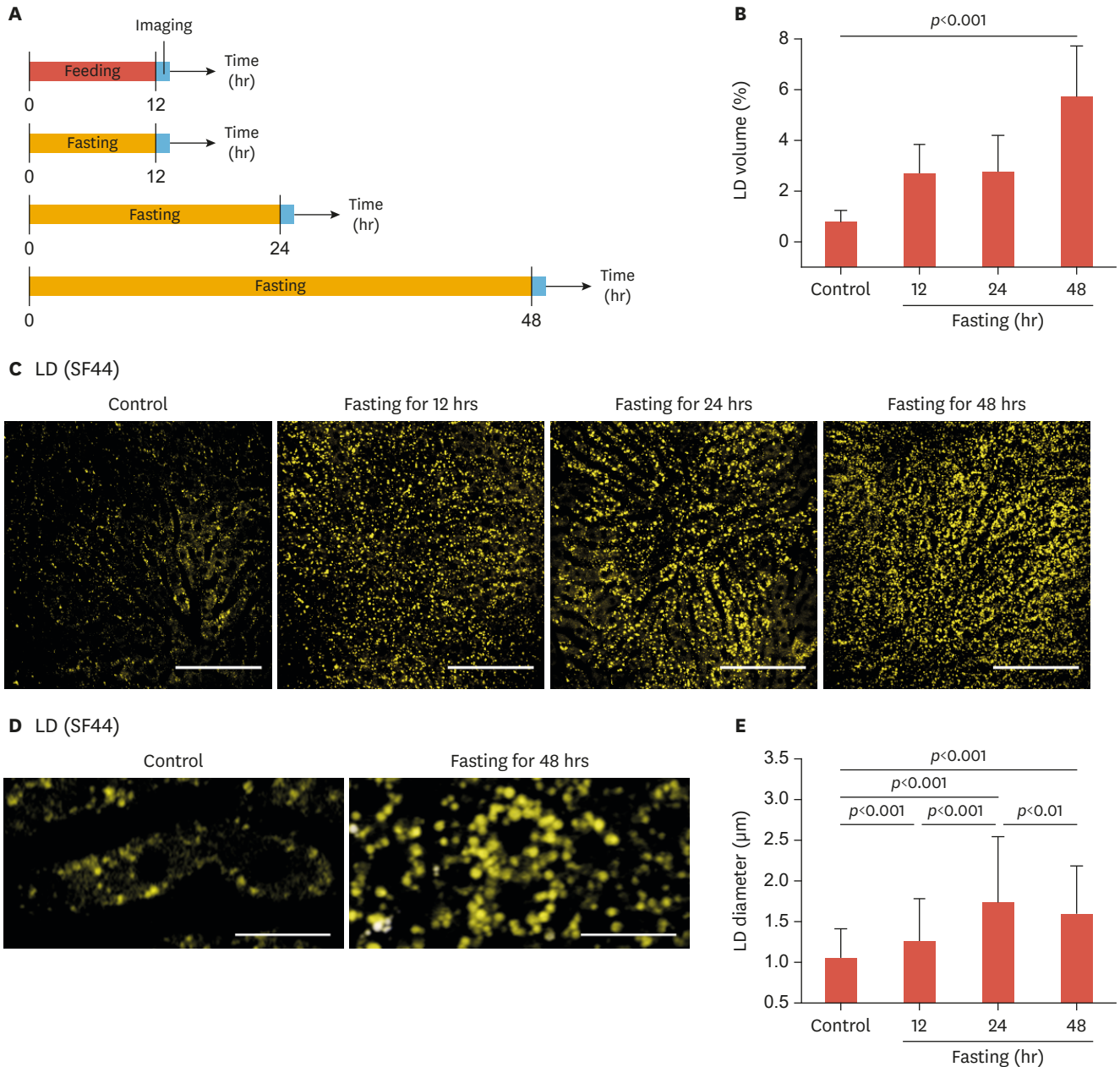


Fig. 2. Intravital imaging of hepatic LDs accumulation induced by fasting. (A) Experimental scheme of intravital liver imaging after normal feeding for 12 hours or fasting for 12, 24, and 48 hours. (B) Quantitative analysis of the volumetric LD ratio in the liver. (C) Representative images of hepatic LDs in the liver of anesthetized mice after normal feeding or fasting. (D) Magnified images of individual LDs in hepatocytes (E) Average diameter of hepatic LDs. Data are presented as mean±standard deviation of mean. Scale bars, (B) 100 μm, (D) 20 μm. LD, lipid droplet; SF44, Seoul-Flour 44.

In the magnified images shown in **Fig. 2D**, the intracellular distribution of the LDs in the hepatocytes of control mice without fasting and mice fasted for 48 hours could be observed. In the control mice, hepatic LDs were sparsely distributed in the cytoplasm of hepatocytes and the nucleus was located in the center of the hepatocyte. After fasting for 48 hours, the number and the size of hepatic LDs were significantly increased and densely accumulated in the cytoplasm of the hepatocyte. However, cellular-level morphological changes such as hepatocyte ballooning or displacement of the nucleus toward the periphery of the hepatocyte, features commonly observed in a pathologic fatty liver, were not observed. **Fig. 2E** shows the average diameter of hepatic LDs observed in the liver of mice without fasting (control) or after fasting of 12, 24, and 48 hours. In the control mice, the average diameter of hepatic LDs was 1.04 μm . In the fasted mice, the average diameter of hepatic LDs increased significantly to 1.19 μm at 12 hours fasting, and then further increased to 1.69 μm at 24 hours fasting. Finally, after 48 hours of fasting, the increased average LD diameter declined slightly to 1.54 μm . With fasting up to 48 hours, hepatic LD accumulation was progressed by continuous increases in the number of LDs not in the size of individual LDs.

2. Intravital 2-photon imaging of the resolution of fasting-induced hepatic LD accumulation with refeeding

To further explore whether the fasting-induced hepatic steatosis was reversible with refeeding, repetitive intravital 2-photon liver imaging of the same mice after fasting and refeeding was performed as depicted in **Fig. 3A**. We performed the first intravital imaging after fasting for 24

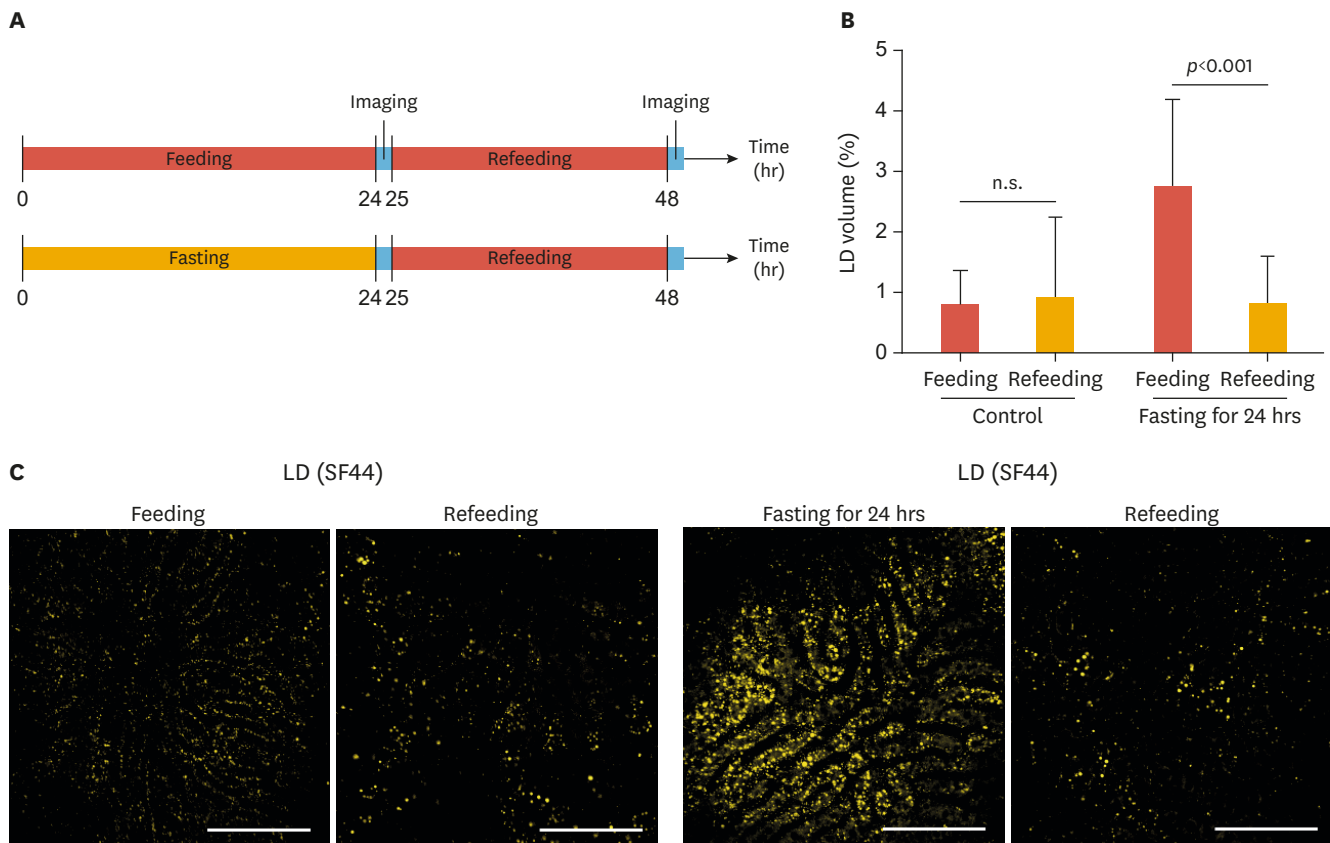


Fig. 3. Intravital imaging of resolution of accumulated hepatic LDs with refeeding after fasting. (A) Experimental scheme of the repeated intravital liver imaging of the same mice after fasting and refeeding. (B) Quantitative analysis of the volumetric LD ratio in the liver. (C) Representative images of hepatic LDs in the liver after normal feeding or fasting and refeeding. Data are presented as mean±standard deviation of mean. Scale bars, 100 μm . LD, lipid droplet; SF44, Seoul-Flour 44.

hours and then the second intravital imaging was performed after the mice were refed a normal diet for 24 hours. As demonstrated in **Fig. 2B**, the first imaging after 24 hours of fasting revealed significantly increased hepatic LDs in the liver (**Fig. 3B and C**). The volumetric LDs ratio in the liver after 24 hours of fasting was much higher, 2.78%, in comparison with that (0.82%) in the liver of normally fed mice. However, after 24 hours of refeeding, the second imaging of the same mice revealed that the accumulated hepatic LDs almost completely disappeared and the volumetric ratio of hepatic LDs was reduced to a similar level to that of the control mice (0.93% and 0.83% in the control mice and the fasted-refed mice, respectively).

DISCUSSION

Although alteration of LDs in the liver by nutritional stress has been previously observed by common *ex vivo* or *in vitro* imaging techniques,¹⁹ a detailed *in vivo* analysis to unveil temporal dynamics of LDs in the same mice at different states has been challenging. In this study, we successfully visualized a highly dynamic *in vivo* changes in hepatic LDs during fasting and refeeding in the same mice by using a custom-built high-resolution intravital 2-photon microscopy system. SF44, a newly developed fluorescence dye for LD labeling,^{20,21} was used to systemically label LDs *in vivo* by intravenous tail-vein injection.¹¹ A recent study revealed that the intravenously injected SF44 was quickly absorbed in the hepatocytes and then specifically labeled LDs in the cytoplasm of hepatocytes within 10 minutes.¹¹ Furthermore, the absorbed SF44 was almost completely cleared out from the hepatocytes after 4 hours,¹¹ which allowed repeated intravital imaging of the liver of the same mouse at later time points.

By intravital liver imaging of hepatic LDs deposition after fasting for maximum 48 hours, we successfully visualized continuous *in vivo* accumulation of hepatic LDs, mostly due to excessive influx of FAs released from adipocytes in various adipose tissue into blood circulation (**Fig. 2C**). Additionally, with subcellular-level high-resolution imaging (**Fig. 2D**), we showed that the increases in the number of microvesicular LDs with an average diameter smaller than 2 μm resulted in a substantially increased volumetric ratio of hepatic LDs in the liver (**Fig. 2B and E**). Notably, in several pathological conditions such as obesity, type 2 diabetes and nonalcoholic fatty liver disease (NAFLD), enlarged hepatocytes due to intracellular accumulation of large LDs in the cytoplasm were commonly observed as a hallmark of pathological liver.²² Accumulation of large LDs in the cytoplasm of hepatocytes could induce a displacement of the nucleus from the center to the periphery of the hepatocyte as NAFLD progressed.²³ However, as shown in **Fig. 2D**, no such pathological morphologic changes of hepatocytes were observed with hepatic LDs accumulation induced by 48 hours fasting. Furthermore, repeated intravital liver imaging of the same mice during fasting and refeeding revealed that the fasting-induced hepatic LD accumulation was fully resolved after refeeding for 24 hours to a similar level to the baseline in the liver of normally fed mice (**Fig. 3B and C**).

This work showed that hepatic LDs accumulation induced by fasting up to 48 hours is a transient, reversible state that can be recovered to the normal state after resupply of the normal diet. Remarkably, by utilizing a custom-built 2-photon intravital microscopy system with a newly developed *in vivo* LD labeling fluorophore, SF44, highly dynamic changes of LDs deposition in hepatocytes during fasting and refeeding were successfully visualized. In the lipid research field, various pathways involved in lipid metabolism or lipidomic analysis in pre-pathological and pathological conditions such as obesity, metabolic syndrome, diabetes, and NAFLD have been actively studied.^{5,24-26} The newly established intravital imaging methods

of LDs in *in vivo* physiological and pathological microenvironments demonstrated in our study will provide a highly useful tool for future investigations to explore novel molecular and cellular mechanisms involving lipid in physiological and various pathological conditions or to assess novel treatment strategies to alleviate deposition of lipids in preclinical animal models.

REFERENCES

1. Nguyen P, Leray V, Diez M, Serisier S, Le Bloc'h J, Siliart B, et al. Liver lipid metabolism. *J Anim Physiol Anim Nutr (Berl)* 2008;92:272-283.
[PUBMED](#) | [CROSSREF](#)
2. Cahill GF Jr. Fuel metabolism in starvation. *Annu Rev Nutr* 2006;26:1-22.
[PUBMED](#) | [CROSSREF](#)
3. Hashimoto T, Cook WS, Qi C, Yeldandi AV, Reddy JK, Rao MS. Defect in peroxisome proliferator-activated receptor α -inducible fatty acid oxidation determines the severity of hepatic steatosis in response to fasting. *J Biol Chem* 2000;275:28918-28928.
[PUBMED](#) | [CROSSREF](#)
4. Guan HP, Goldstein JL, Brown MS, Liang G. Accelerated fatty acid oxidation in muscle averts fasting-induced hepatic steatosis in SJL/J mice. *J Biol Chem* 2009;284:24644-24652.
[PUBMED](#) | [CROSSREF](#)
5. Chitraju C, Trötz Müller M, Hartler J, Wolinski H, Thallinger GG, Lass A, et al. Lipidomic analysis of lipid droplets from murine hepatocytes reveals distinct signatures for nutritional stress. *J Lipid Res* 2012;53:2141-2152.
[PUBMED](#) | [CROSSREF](#)
6. Heijboer AC, Donga E, Voshol PJ, Dang ZC, Havekes LM, Romijn JA, et al. Sixteen hours of fasting differentially affects hepatic and muscle insulin sensitivity in mice. *J Lipid Res* 2005;46:582-588.
[PUBMED](#) | [CROSSREF](#)
7. Rubart M. Two-photon microscopy of cells and tissue. *Circ Res* 2004;95:1154-1166.
[PUBMED](#) | [CROSSREF](#)
8. Pittet MJ, Weissleder R. Intravital imaging. *Cell* 2011;147:983-991.
[PUBMED](#) | [CROSSREF](#)
9. Germain RN, Robey EA, Cahalan MD. A decade of imaging cellular motility and interaction dynamics in the immune system. *Science* 2012;336:1676-1681.
[PUBMED](#) | [CROSSREF](#)
10. Ellenbroek SJJ, van Rheenen J. Imaging hallmarks of cancer in living mice. *Nat Rev Cancer* 2014;14:406-418.
[PUBMED](#) | [CROSSREF](#)
11. Moon J, Kong E, Lee J, Jung J, Kim E, Park SB, et al. Intravital longitudinal imaging of hepatic lipid droplet accumulation in a murine model for nonalcoholic fatty liver disease. *Biomed Opt Express* 2020;11:5132-5146.
[PUBMED](#) | [CROSSREF](#)
12. Lee J, Kong E, Hong S, Moon J, Kim P. *In vivo* longitudinal visualization of the brain neuroinflammatory response at the cellular level in LysM-GFP mice induced by 3-nitropropionic acid. *Biomed Opt Express* 2020;11:4835-4847.
[PUBMED](#) | [CROSSREF](#)
13. Park I, Kim M, Choe K, Song E, Seo H, Hwang Y, et al. Neutrophils disturb pulmonary microcirculation in sepsis-induced acute lung injury. *Eur Respir J* 2019;53:1800786.
[PUBMED](#) | [CROSSREF](#)
14. Thorling CA, Crawford D, Burczynski FJ, Liu X, Liao I, Roberts MS. Multiphoton microscopy in defining liver function. *J Biomed Opt* 2014;19:90901.
[PUBMED](#) | [CROSSREF](#)
15. Sekimoto R, Fukuda S, Maeda N, Tsushima Y, Matsuda K, Mori T, et al. Visualized macrophage dynamics and significance of S100A8 in obese fat. *Proc Natl Acad Sci U S A* 2015;112:E2058-E2066.
[PUBMED](#) | [CROSSREF](#)
16. Park I, Choe K, Seo H, Hwang Y, Song E, Ahn J, et al. Intravital imaging of a pulmonary endothelial surface layer in a murine sepsis model. *Biomed Opt Express* 2018;9:2383-2393.
[PUBMED](#) | [CROSSREF](#)
17. Hwang Y, Yoon H, Choe K, Ahn J, Jung JH, Park JH, et al. *In vivo* cellular-level real-time pharmacokinetic imaging of free-form and liposomal indocyanine green in liver. *Biomed Opt Express* 2017;8:4706-4716.
[PUBMED](#) | [CROSSREF](#)

18. Ahn S, Choe K, Lee S, Kim K, Song E, Seo H, et al. Intravital longitudinal wide-area imaging of dynamic bone marrow engraftment and multilineage differentiation through nuclear-cytoplasmic labeling. *PLoS One* 2017;12:e0187660.
[PUBMED](#) | [CROSSREF](#)
19. Kramer DA, Quiroga AD, Lian J, Fahlman RP, Lehner R. Fasting and refeeding induces changes in the mouse hepatic lipid droplet proteome. *J Proteomics* 2018;181:213-224.
[PUBMED](#) | [CROSSREF](#)
20. Kim E, Lee Y, Lee S, Park SB. Discovery, understanding, and bioapplication of organic fluorophore: a case study with an indolizine-based novel fluorophore, Seoul-Fluor. *Acc Chem Res* 2015;48:538-547.
[PUBMED](#) | [CROSSREF](#)
21. Kim E, Lee S, Park SB. A Seoul-Fluor-based bioprobe for lipid droplets and its application in image-based high throughput screening. *Chem Commun (Camb)* 2012;48:2331-2333.
[PUBMED](#) | [CROSSREF](#)
22. Caldwell S, Ikura Y, Dias D, Isomoto K, Yabu A, Moskaluk C, et al. Hepatocellular ballooning in NASH. *J Hepatol* 2010;53:719-723.
[PUBMED](#) | [CROSSREF](#)
23. Takahashi Y, Fukusato T. Histopathology of nonalcoholic fatty liver disease/nonalcoholic steatohepatitis. *World J Gastroenterol* 2014;20:15539-15548.
[PUBMED](#) | [CROSSREF](#)
24. Kim GT, Kim SJ, Park SH, Lee D, Park TS. Hepatic expression of the serine palmitoyltransferase subunit *sptlc2* reduces lipid droplets in the liver by activating VLDL secretion. *J Lipid Atheroscler* 2020;9:291-303.
[PUBMED](#) | [CROSSREF](#)
25. Nishikawa S, Doi K, Nakayama H, Uetsuka K. The effect of fasting on hepatic lipid accumulation and transcriptional regulation of lipid metabolism differs between C57BL/6J and BALB/cA mice fed a high-fat diet. *Toxicol Pathol* 2008;36:850-857.
[PUBMED](#) | [CROSSREF](#)
26. Montagner A, Polizzi A, Fouché E, Ducheix S, Lippi Y, Lasserre F, et al. Liver PPAR α is crucial for whole-body fatty acid homeostasis and is protective against NAFLD. *Gut* 2016;65:1202-1214.
[PUBMED](#) | [CROSSREF](#)